Small Signal Audio Susceptibility Analysis of Flyback Converter With Peak Current Mode Control

Ekrem Çengelci[1]

ABSTRACT

Small signal audio susceptibility of flyback converter with peak current mode control method is presented by utilizing pwm-switch model in Continuous Conduction Mode (CCM). The analysis provides input voltage to output voltage transfer function together with its zeros and poles in symbolic form. Numerator and denominator of the resultant transfer function are both 3rd order. While symbolic equations of zeros are provided as exact solutions, the symbolic equations of poles are provided as approximate solutions with the assumption that the real pole is well separated from the resonant frequency of the complex pole pair. Symbolically derived transfer function of flyback converter is validated on a numerical example by time domain PSIM simulations on a switching flyback converter model. The mathematical analysis and PSIM simulations of input voltage to output voltage transfer function of the converter agree very well up to frequencies below half the switching frequency.

Keywords: dc/dc Flyback converter, pwm-switch, peak current mode control, small signal analysis

1. INTRODUCTION

Flyback converter is a popular switching dc/dc converter topology in relatively low power applications with the advantages of providing galvanic isolation between input and output with smallest power components count [1].

Current mode control [2] is widely used with switching power converters with several advantages [3] such as eliminating phase-lag from control voltage to the switch/inductor current, inherent pulse-by-pulse current limiting protecting the converter against overloads, ease of paralleling converter outputs, ease of applying output current feed-forward minimizing output voltage deviations under load transients, inherent sensitivity to static and dynamic variations of input voltage.

Some switching dc/dc converter applications, such as test and measurement, medical equipment,

communication equipment, base stations and many others, require to have high input ripple voltage rejection at the converter output. Small signal transfer function from input voltage to output voltage of the converter (audio susceptibility) is required to evaluate input voltage rejection performance of a switching converters. Audio susceptibility differs depending on the power topology, conduction and control modes.

In this paper, input voltage to output voltage transfer function of flyback converter is presented in symbolic form with peak current mode control in CCM employing the pwm-switch model in [4]-[6]. Symbolic equations of zeros and poles of the transfer function are derived, which provides physical insight to the audio susceptibility of the flyback converter topology. The transfer function has a 3rd order numerator and 3rd order denominator with one real zero, one real pole, a complex zero pair and a complex pole pair. The real zero factors out in the numerator enabling to derive

[1] TÜBİTAK MAM, Turkey ekrem.cengelci@tubitak.gov.tr

exact equations for the location of the real zero, resonant frequency and quality factor of the complex zero pair. On the other hand, the real pole doesn't factor out in the denominator that requires the assumption of the real pole being well separated from the resonant frequency of the complex pole pair to derive approximate equations for the location of the real pole, resonant frequency and quality factor of the complex pole pair.

The symbolic transfer function derived in the paper is validated on an example flyback converter
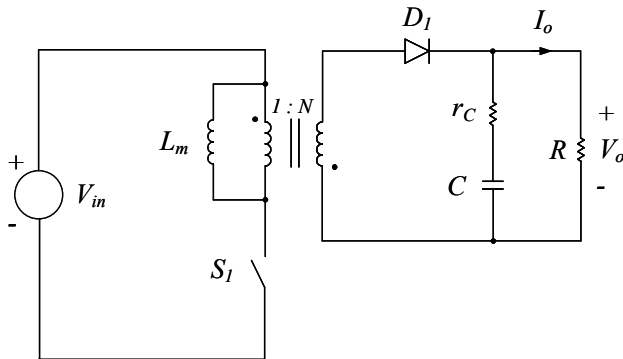

Figure 1. Circuit diagram of flyback converter.

by time domain PSIM simulations. Bode plots of the example converter are generated utilizing the symbolic transfer function provided and compared to the Bode plots obtained through time domain PSIM simulations. Both Bode plots agree very well at low and medium frequencies and depart from each other as frequency approaches half the switching frequency. The symbolic equations of zeros and poles provided enable designers to optimize the audio susceptibility at the stage of determining the close loop control parameters of flyback converter with peak current mode control in CCM.

2. PWM SWITCH MODEL WITH PEAK CURRENT MODE CONTROL IN CCM

Pwm-switch models presented in [4]-[6] enable circuit-oriented small signal analysis of switching dc/dc converters. It represents the switch pair in a dc/dc converter with three terminals, which are active terminal "a", passive terminal "p" and common terminal "c". The pwm-switch model has dc, large signal and small signal models. Fig. 2 shows significant control signal waveforms, the dc and small signal ac circuit diagrams of the pwm-switch model with peak current-mode control in CCM [5], [6]. In Fig. 2b, upper case voltages and currents represent dc operating point quantities of the converter while lower case ones with tilde

accent marks represent small signal ac quantities of the converter. The dc model is utilized to solve for dc operating point quantities while the ac model facilitates to determine the desired small signal transfer function of the dc/dc converter to be analyzed, such as control to output voltage or input to output voltage transfer functions, input or output impedances.

Equations of the pwm-switch model parameters in Fig. 2 are shown in (1) below.
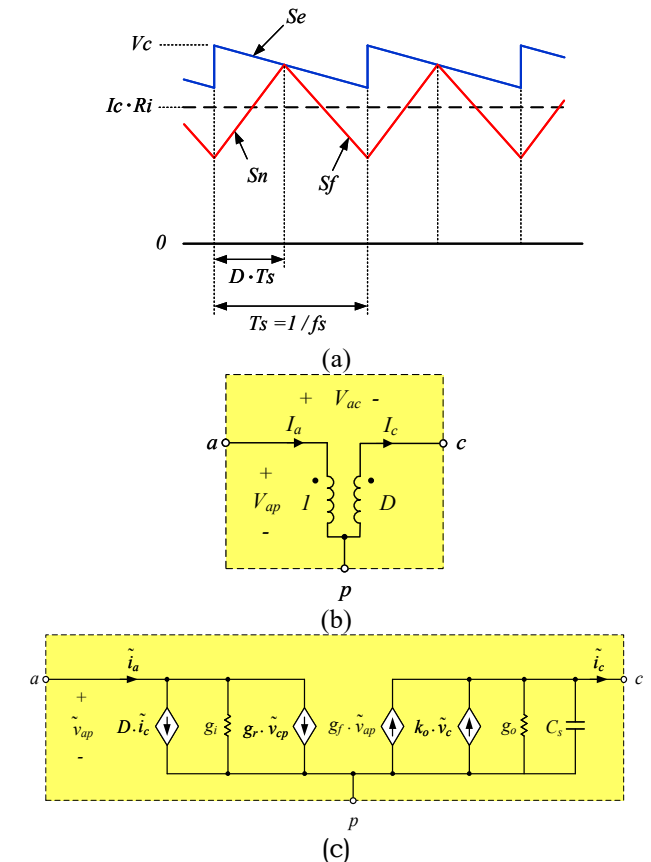

(a)

(b)

(c)

Figure 2. Pwm-switch model with peak current-mode control in CCM (a) Significant control signal waveforms (b) dc equivalent circuit (c) ac equivalent circuit.

$$k_o = \frac{1}{R_i} \qquad g_o = \frac{T_s}{L_m} \cdot \left(D' \frac{S_e}{S_n} + 0.5 - D \right)$$

$$g_f = D \cdot g_o - \frac{D \cdot D' \cdot T_s}{2 \cdot L_m} \qquad g_i = -\frac{I_a}{V_{ap}}$$

$$g_r = \frac{I_c}{V_{ap}} \qquad C_s = \frac{4}{L_m \cdot \left(\frac{2\pi}{T_s} \right)^2} \qquad (1)$$

where,

R_i is a scaling constant that transforms the "c" terminal current to voltage signal (Ω),

D is the duty cycle in steady state and $D' = 1 - D$,

T_s is the switching period (s),

$$S_n = \frac{V_{ac}}{L_m} \cdot R_i \text{ (V/s)} \qquad S_f = \frac{V_{cp}}{L_m} \cdot R_i \text{ (V/s)} \qquad (2)$$

S_e is slope of the external compensation signal (V/s).

Sakarya University Journal of Science, 22(4): 1157-1162, 2018.

1158

Note that S_n and S_f are up slope and down slope of the current coming out of terminal "c" as reflected to the control voltage by the scaling constant R_i. The capacitor C_s in Fig. 2c is to model the subharmonic instability of the current loop [5], [6].

The steady state value of control voltage V_c (Fig. 2a) can be solved using (3) below (see [6] for details).

$$I_c = \frac{V_c}{R_i} - \frac{V_{cp}}{V_{ap}} \cdot \frac{T_s \cdot S_e}{R_i} - V_{cp} \cdot \left(1 - \frac{V_{cp}}{V_{ap}}\right) \cdot \frac{T_s}{2 \cdot L_m} \quad (3)$$

3. INPUT VOLTAGE TO OUTPUT VOLTAGE TRANSFER FUNCTION OF FLYBACK CONVERTER WITH PEAK CURRENT MODE CONTROL IN CCM

To utilize the pwm-switch model in Fig. 2 in analysis of flyback converter, the switch S_1 and diode D_1 in Fig. 1 need to be connected at a common terminal. Therefore, the flyback topology in Fig. 1 needs to be changed around to represent the flyback topology with pwm-switch model without altering the circuit operation.

Representation of flyback converter with the pwm-switch model is given in [7] and shown in Fig. 3.
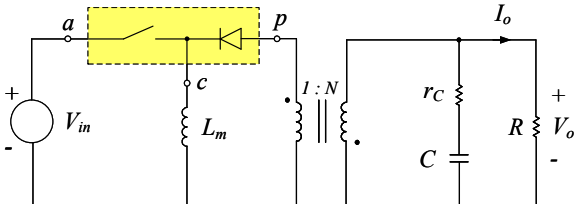

Figure 3. Representation of flyback converter by the pwm-switch model

To solve for the pwm-switch model parameters in (1), we need to obtain dc equivalent circuit of flyback converter by substituting the dc pwm-switch model in Fig. 2b into the switch pair shown within dotted box in Fig. 3. After shorting the output capacitor and opening the magnetizing inductor, the circuit parameters D, I_a, I_c, V_{ap} and V_{ac} in (1) and (2) are solved using the resultant dc equivalent circuit, which is shown in Fig. 4.
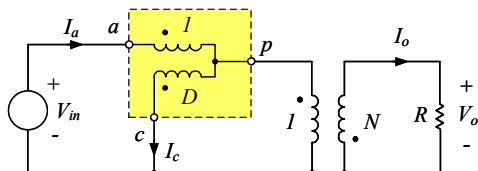

Figure 4. Dc pwm-switch equivalent circuit of flyback converter in Fig. 3.

If D, I_a, I_c, V_{ap} and V_{ac} are solved from Fig. 4 and substituted into (1) and (2), equations in (4) can be obtained as shown below.

$$\frac{V_o}{V_{in}} = N \cdot \frac{D}{1-D} \qquad D = \frac{1}{1+N \cdot \frac{V_{in}}{V_o}} \qquad V_{ap} = \frac{V_o}{N \cdot D}$$

$$I_c = N \cdot \frac{I_o}{(1-D)} \qquad I_a = N \cdot I_o \cdot \frac{D}{(1-D)} \qquad V_{ac} = V_{in}$$

$$V_{cp} = \frac{V_o}{N} \qquad g_i = -\frac{D^2 \cdot N^2}{R \cdot (1-D)} \qquad g_r = \frac{D \cdot N^2}{R \cdot (1-D)}$$

$$S_n = V_{in} \cdot \frac{R_i}{L_m} \qquad S_f = \frac{V_o}{N} \cdot \frac{R_i}{L_m} \qquad (4)$$

Using (3) and (4) the control voltage V_c can be solved as given in (5).

$$V_c = \frac{R_i \cdot V_o \cdot (1-D)}{2 \cdot N \cdot L_m \cdot fs} + \frac{N \cdot R_i \cdot I_o}{(1-D)} + \frac{D \cdot S_e}{f_s} \quad (5)$$

The next step is to obtain the ac equivalent circuit of flyback converter to solve for the transfer function of $\tilde{v}_o(s)/\tilde{v}_{in}(s)$. The ac equivalent circuit of flyback converter is obtained by substituting the ac pwm-switch model in Fig. 2c into the switch pair shown within dotted box in Fig. 3. Note that the current source $k_o \cdot \tilde{v}_c$ in Fig. 2c is removed in Fig. 5 since the perturbation control signal $\tilde{v}_c$ is needed to derive the transfer function from the control signal to output voltage. To derive the audio susceptibility transfer function of flyback converter, the perturbation voltage signal $\tilde{v}_{in}$ is placed at the input of the converter in Fig. 5. The circuit in Fig. 5 can be solved by linear circuit analysis methods to derive the audio susceptibility transfer function $\tilde{v}_o(s)/\tilde{v}_{in}(s)$ as given in (6) below.
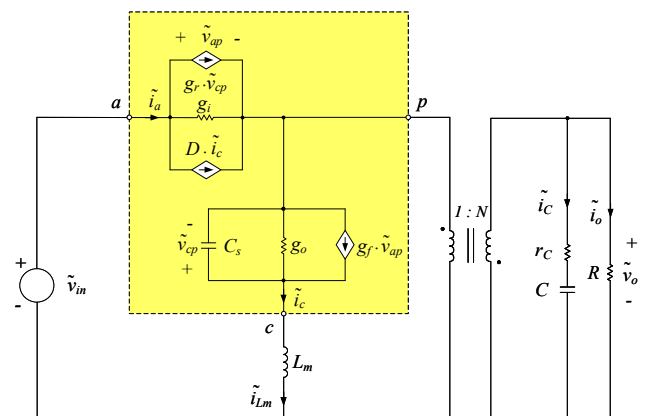

Figure 5. Ac small signal pwm-switch model of flyback converter.

$$\frac{\tilde{v}_o(s)}{\tilde{v}_{in}(s)} = -R \cdot N \cdot \frac{\left(1+\frac{s}{\omega_{z1}}\right)\left(\begin{array}{c} g_i-(1-D) \cdot g_f+ \\ (g_f \cdot g_r+g_i \cdot g_o) \cdot L_m \cdot s+ \\ C_s \cdot L_m \cdot g_i \cdot s^2 \end{array}\right)}{D_0+D_1 \cdot s+D_2 \cdot s^2+D_3 \cdot s^3} \quad (6)$$

where,

$$D_0 = N^2 + R \cdot [g_i + g_r + (g_o - g_f) \cdot (1-D)]$$

$D_1 = N^2 \cdot (g_o \cdot L_m + r_C \cdot C) +$
$\quad R \cdot [(1-D) \cdot C_s + (g_r \cdot g_f + g_i \cdot g_o) \cdot$
$\quad L_m + C \cdot [N^2 + r_C \cdot (g_i + g_r + (g_o - g_f) \cdot$
$\quad (1-D))]]$

$D_2 = L_m \cdot N^2 (C_s + C \cdot g_o \cdot r_C) + R \cdot [(1-D) \cdot$
$\quad C_s \cdot r_C \cdot C + L_m \cdot [g_i \cdot C_s + C \cdot [N^2 \cdot g_o + r_C \cdot$
$\quad (g_r \cdot g_f + g_i \cdot g_o)]]]$

$D_3 = L_m \cdot C \cdot C_s \cdot [R \cdot r_C \cdot g_i + N^2 \cdot (R + r_C)]$

If (6) is reorganized in the form of poles and zeros, it can be re-expressed as given in (7) below.

$$\frac{\tilde{v}_o(s)}{\tilde{v}_{in}(s)} = K_{dc} \cdot \frac{\left(1+\frac{s}{\omega_{z1}}\right)\cdot\left(1+\frac{s}{Q_z\cdot\omega_z}+\frac{s^2}{\omega_z^2}\right)}{\left(1+\frac{s}{\omega_{p1}}\right)\cdot\left(1+\frac{s}{Q_p\cdot\omega_p}+\frac{s^2}{\omega_p^2}\right)} \quad (7)$$

where,

$$\omega_{z1} = \frac{1}{C\cdot r_C} \qquad K_{dc} = \frac{-R\cdot N\cdot(g_i-(1-D)\cdot g_f)}{N^2+R\cdot[g_i+g_r+(g_o-g_f)\cdot(1-D)]}$$

$$\omega_z = \sqrt{\frac{g_i-(1-D)\cdot g_f}{C_s\cdot L_m\cdot g_i}} \cong \pi\cdot f_s$$

$$Q_z = \frac{\sqrt{C_s\cdot L_m\cdot g_i\cdot(g_i-(1-D)\cdot g_f)}}{L_m\cdot(g_r\cdot g_f+g_i\cdot g_o)}$$

$$\omega_{p1} \cong \frac{D_0}{D_1} \quad \omega_p \cong \sqrt{\frac{D_1}{D_3}} \cong \pi\cdot f_s \quad Q_p \cong \frac{\sqrt{D_1\cdot D_3}}{D_2} \quad (8)$$

Note that the denominator of (6) is third order and the poles can be expressed only as approximate solutions (see [8]) assuming there is a real pole at low frequency and a complex pole pair with a resonant frequency at a significantly higher frequency (10 times or higher). (7) represents the poles of (6) as approximate solutions with approximate equations of ω_{p1}, ω_p, and Q_p given in (8). The accuracies of equations for ω_{p1}, ω_p and Q_p increase as the ratio of ω_p/ω_{p1} increases.

By substituting (4) into (8), K_{dc}, ω_z and ω_{p1} can be expressed as,

$$K_{dc} = \frac{R\cdot T_s\cdot N\cdot D\cdot(1-D)^2\cdot[2\cdot S_e\cdot(1-D)-S_n\cdot D]+2\cdot D^2\cdot L_m\cdot N^3\cdot S_n}{R\cdot T_s\cdot(1-D)^4\cdot(S_n+2\cdot S_e)+2\cdot L_m\cdot N^2\cdot S_n\cdot(1-D^2)}$$

$$\omega_{p1} \xrightarrow[\substack{r_C=0, \\ C_s=0}]{} \frac{R\cdot T_s\cdot(1-D)^3\cdot(S_n+2\cdot S_e)+2\cdot L_m\cdot N^2\cdot S_n\cdot(1+D)}{L_m\cdot N^2\cdot[2\cdot T_s\cdot S_e\cdot(1-D)+2\cdot C\cdot R\cdot S_n-T_s\cdot S_n\cdot(D^2+2\cdot D-1)]}$$

$$\omega_z = \sqrt{\frac{(1-D)^2\cdot[(1-D)\cdot S_e-S_n\cdot\frac{D}{2}]\cdot T_s\cdot R}{C_s\cdot D\cdot S_n\cdot L_m^2\cdot N^2}+\frac{1}{C_s\cdot L_m}} \quad (9)$$

4. SIMULATION RESULTS

In this section, the transfer function $\tilde{v}_o(s)/\tilde{v}_{in}(s)$ derived analytically for the flyback converter with peak current mode control in CCM will be proven by time domain PSIM simulations on a switching flyback converter model.

Consider a flyback converter with parameters below.

$V_{in} = 5V \qquad V_o = 15V \qquad I_o = 2A$

$R = 7.5\Omega \quad f_s = 500kHz \quad \omega_s = 3.141Mrad/s$

$R_i = 50m\Omega \qquad C = 330\mu F \qquad r_C = 30m\Omega$

$L_m = 2\mu H \qquad Se = 140kV/s \qquad N = 2$

The magnetizing inductance L_m is chosen such that the peak to peak ripple current of magnetizing inductor is about 30% of its average current. Using (1), (2), (5), and (8) the following parameters can be calculated.

$D = 0.6 \quad g_o = 0.348mho \quad g_f = 0.0888mho$

$g_i = -0.48mho \quad g_r = 0.8mho \quad C_s = 203nF$

$S_n = 125kV/s \qquad S_f = 187.5kV/s$

$K_{dc} = 1.077 \qquad V_c = 0.743V$

Fig. 6 shows time domain PSIM simulation model of the example flyback converter with open loop control. Fig. 7 shows the time domain simulation waveforms of the flyback converter in Fig. 6. In Fig. 7, the waveforms from top to bottom in order are output voltage, magnetizing inductor current, voltage of external slope signal, input voltage of pwm comparator, and gate signal of the power switch.

The control voltage V_c in Fig. 6 varies with output voltage and current as given in (5). V_c is calculated 0.743V by (5), which sets the output voltage to 15V as shown in Fig. 7.

The audio susceptibility transfer function given in (6) can be calculated for the example flyback converter as given in (10) below.

$$\frac{\tilde{v}_o(s)}{\tilde{v}_{in}(s)} = 1.077 \cdot \frac{1+1.027\cdot10^{-5}\cdot s+4.065\cdot10^{-12}\cdot s^2+3.736\cdot10^{-18}\cdot s^3}{1+1.389\cdot10^{-3}\cdot s+9.627\cdot10^{-10}\cdot s^2+5.592\cdot10^{-16}\cdot s^3} \quad (10)$$

If the roots of the numerator and denominator of (10) are solved numerically, (10) can be expressed as shown in (11) below.

$$\frac{\tilde{v}_o(s)}{\tilde{v}_{in}(s)} = 1.077 \cdot \frac{\left(1+\frac{s}{101.01\cdot10^3}\right)\cdot\left[\left(1+\frac{s}{493.5\cdot10^3-1551.3\cdot10^3\cdot j}\right)\cdot\left(1+\frac{s}{493.5\cdot10^3+1551.3\cdot10^3\cdot j}\right)\right]}{\left(1+\frac{s}{720.03}\right)\cdot\left[\left(1+\frac{s}{860.4\cdot10^3-1320.3\cdot10^3\cdot j}\right)\cdot\left(1+\frac{s}{860.4\cdot10^3+1320.3\cdot10^3\cdot j}\right)\right]} \quad (11)$$

It is observed in (11) that the transfer function has one real zero, one real pole, a complex zero pair and a complex pole pair. Table 1 below summarizes the locations of real zero and pole and

quality factors and resonant frequencies of the complex zero pair and complex pole pair.

ω_{z1}, ω_z, and Q_z are given in (8) without any approximation. Therefore, solving these parameters using equations in (8) and the transfer function in (11) yields identical results as shown in Table 1. However, ω_{p1}, ω_p, and Q_p were given in (8) with the assumption that $\omega_p \gg \omega_{p1}$. Since this condition is met with this specific flyback conver-
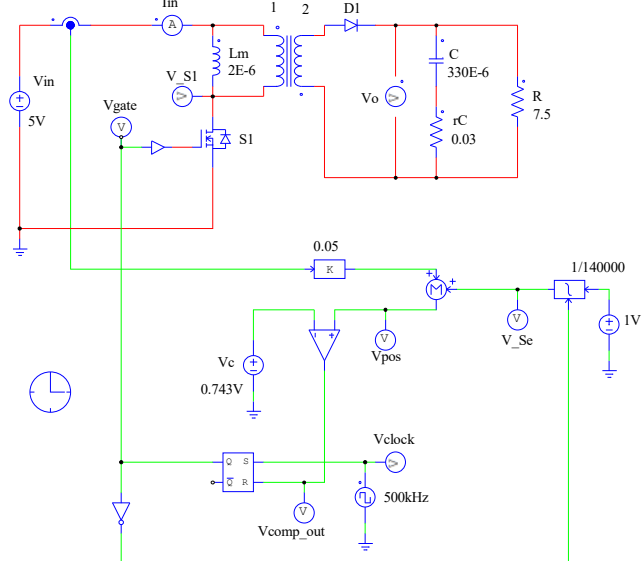
Table 1. Summary of zeros and poles of the example flyback converter.

Parameter	Exact Solutions (Eq. 11)	Approximate Solutions (Eq. 8)	Unit
ω_{z1}	$101.01 \cdot 10^3$		rad/s
ω_z	$1.628 \cdot 10^6$		
Q_z	1.65		
ω_{p1}	720	719.7	rad/s
ω_p	$1.576 \cdot 10^6$	$1.576 \cdot 10^6$	
Q_p	0.915	0.915	

Fig. 8 shows Bode plots of the example flyback converter by PSIM simulation and mathematical analysis. The circuit model in Fig. 6 is used for PSIM simulated Bode plots in Fig. 8. The transfer function in (10) is used for the Bode plots obtained through mathematical analysis in Fig. 8. It is observed in Fig. 8 that Bode plots generated through PSIM and mathematical analysis are very well matched at low and medium frequencies and they differ as the frequency approaches half the switching frequency due to the limitations of small signal mathematical model at high frequencies.

Figure 6. Switching model of the flyback converter for time domain PSIM simulations.

Figure 8. Bode plot comparisons of the example flyback converter as simulated by PSIM and calculated by (10).

5. CONCLUSIONS

Symbolic small signal audio susceptibility of flyback converter with peak current mode control method in CCM is presented by utilizing the pwm-switch model. Input voltage to output voltage transfer function, its real pole and real zero, resonant frequencies and quality factors of complex poles and complex zeros are provided in symbolic form in the paper. While symbolic equations of zeros are provided as exact solutions, the symbolic equations of poles are provided as approximate solutions with the assumption that the real pole is well separated from the resonant frequency of the complex pole pair. Mathematically derived audio susceptibility transfer function of flyback converter is validated on a numerical example by time domain PSIM simulations on a switching flyback converter model. The mathema-
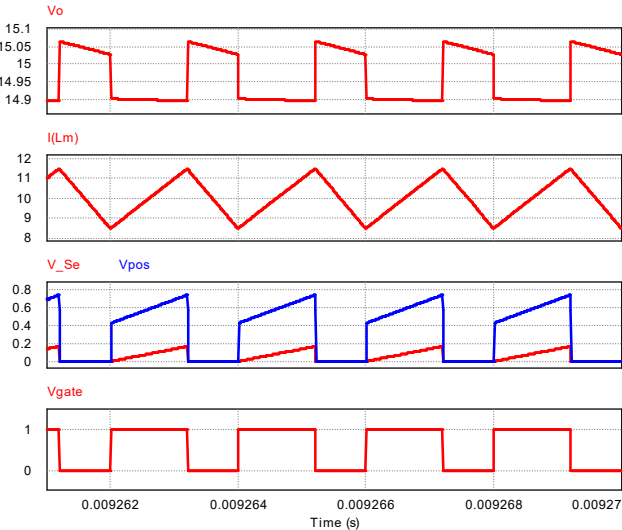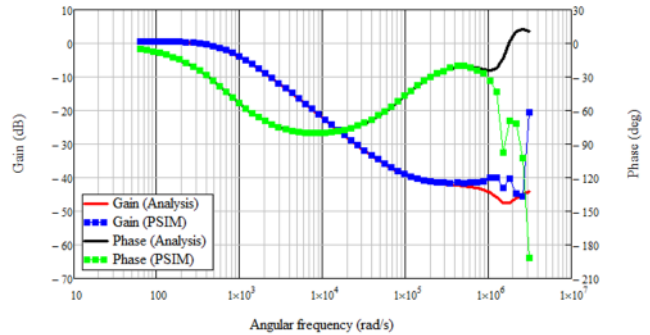

Figure 7. PSIM time domain simulation waveforms of the flyback converter in Fig. 6.

ter example, ω_{p1}, ω_p, and Q_p calculated by approximate equations in (8) and calculated by using (11) for exact solutions yield very close results.

tical analysis and PSIM simulations of input voltage to output voltage transfer function of the example flyback converter agree very well at low and medium frequencies. As the frequency approaches half the switching frequency, PSIM simulation and small signal analysis results do not agree well due to the limitations of the small signal model at high frequencies.

REFERENCES

[1] A. Ioinovici, "Power Electronics and Energy Conversion Systems-Volume I," John Wiley and Sons, Boulder, West Sussex, United Kingdom, 2013.

[2] R. Ridley, "A New Small Signal Model for Current Mode Control", Ph.D. Dissertation, ECE Dept., Virginia Institute of Tech., Blacksburg, VA, USA, 1990.

[3] R. Redl, N. Sokal, "Current-mode control, five different types, used with the three basic classes of power converters", *IEEE PESC*, Toulouse, France, 1985, pp. 771-785.

[4] V. Vorperian, "Simplified analysis of PWM converters using model of PWM switch. Part I: Continuous conduction mode," *IEEE Trans. Aerospace Electron. Syst.*, 1990, vol. 26, issue 3, pp. 490-496.

[5] V. Vorperian, "Analysis of Current-Controlled PWM Converters Using the Model of the Current-Controlled PWM Switch," *PCIM Conference*, 1990, pp. 183-195.

[6] V. Vorperian, "Fast Analytical Techniques for Electrical and Electronic Circuits," 1st ed., Cambridge University Press, Cambridge, United Kingdom, 2002.

[7] C. Basso, "Switch-Mode Power Supplies, Spice Simulations and Practical Designs," 1st ed., McGraw-Hill, USA, 2008.

[8] R.W. Erickson, D. Maksimovic, "Fundamentals of Power Electronics," 2nd ed., Kluwer Academic Publishers, Boulder, CO, 2004.